

We propose the following model for CTX phage secretion. CTX $\phi$ 's homolog of fl pI, Zot, a presumed inner membrane protein (21), interacts with a multimer of the outer membrane protein EpsD and thereby induces opening of this outer membrane channel, through which the phage is released. Additional interactions between Zot, EpsD, and phage coat proteins are also likely; interactions between CTX phage-encoded proteins and proteins of the *eps* apparatus other than EpsD are probably not required. It is not known whether a single EpsD multimer can interact simultaneously with components of both secretory pathways or whether the phage and protein secretory processes compete for access to the outer membrane channel.

Phage exploitation of a host secretin has not been demonstrated previously; however, analyses of the genomes of additional filamentous phages suggest that reliance upon a chromosome-encoded secretin may be a common strategy for phage secretion. Within the GenBank database, there are at least five filamentous phages other than CTX $\phi$ —fs1, Vf12, Vf33, Cf1c, and Pf1—that do not appear to encode a pIV homolog and thus may rely upon a chromosomal protein instead. All these phages infect bacterial species that contain type II secretion systems. In contrast, the filamentous coliphages that encode a phage-specific secretin infect a host that generally does not produce a secretory apparatus (22). Thus, coliphages may have been constrained during their evolution to rely upon a phage-encoded secretin. Alternatively, phage-encoded secretins may grant access to a broader range of host species or confer some other evolutionary advantage.

It is somewhat surprising that EpsD can mediate both CTX $\phi$  and CT secretion. Most secretins are unable to function within heterologous systems, even systems composed of very similar proteins with highly related substrates (9, 23). Furthermore, the two secretory processes to which EpsD contributes are markedly different. Phage export releases a cytoplasmic DNA molecule coated with inner membrane-derived coat proteins, whereas type II secretion systems export only free, periplasmic proteins. Nonetheless, in *V. cholerae*, these two disparate classes of secretion substrates both appear to pass through an outer membrane pore composed of EpsD. The convergence of phage and protein secretion pathways may be a clue that structurally similar periplasmic complexes are assembled during each process. Indirect evidence in support of this hypothesis has already been provided by the findings that both pathways bear similarities, at either the sequence or structural level, to type IV pilus assembly (2). Our finding that a filamentous phage and a type II secretion apparatus use the same secretin provides additional evidence that the two export systems have a common evolutionary origin and suggests that they may still maintain mechanistic similarities.

References and Notes

1. B. B. Finlay and S. Falkow, *Microbiol. Mol. Biol. Rev.* **61**, 136 (1997).
2. M. Russel, *J. Mol. Biol.* **279**, 485 (1998).
3. P. J. Christie, *J. Bacteriol.* **179**, 3085 (1997).
4. R. Binet, S. Letoffe, J. M. Ghigo, P. Deleplaire, C. Wandersman, *Gene* **192**, 7 (1997).
5. K. J. Fullner and J. J. Mekalanos, *Infect. Immun.* **67**, 1393 (1999).
6. M. K. Waldor and J. J. Mekalanos, *Science* **272**, 1910 (1996).
7. D. K. Marciano, M. Russel, S. M. Simon, *Science* **284**, 1516 (1999).
8. M. Russel, *Trends Microbiol.* **3**, 223 (1995).
9. ———, *J. Mol. Biol.* **231**, 689 (1993).
10. We searched the *V. cholerae* database with the Institute for Genome Research's BLAST Search Engine for Unfinished Microbial Genomes ([www.tigr.org/cgi-bin/BlastSearch/blast.cgi](http://www.tigr.org/cgi-bin/BlastSearch/blast.cgi)).
11. M. Sandkvist et al., *J. Bacteriol.* **179**, 6994 (1997).
12. J. B. Kaper, J. G. Morris Jr., M. M. Levine, *Clin. Microbiol. Rev.* **8**, 48 (1995).
13. The targeting vector is described by A. Ali et al., *Infect. Immun.* **68**, 1967 (2000).
14. B. M. Davis, E. H. Lawson, M. Sandkvist, M. K. Waldor, H. H. Kimsey, unpublished data.
15. G. D. Pearson, A. Woods, S. L. Chiang, J. J. Mekalanos, *Proc. Natl. Acad. Sci. U.S.A.* **90**, 3750 (1993).
16. C. C. Hase and R. A. Finkelstein, *J. Bacteriol.* **173**, 3311 (1991).
17. *EpsD* (base pairs 1159 to 3245 of the *eps* gene cluster; GenBank accession number L33796) was cloned into the Cm<sup>R</sup>, isopropyl- $\beta$ -D-thiogalactopyranoside (IPTG)-inducible plasmid pGZ119HE (24).
18. M. Judson and J. J. Mekalanos, unpublished data.
19. pMS43 and pMS42 are equivalent to pMS27 and pMS12 (25), except that they are Cm<sup>R</sup>.
20. pCTX-Kn is a more stable replicon than pCTX-Ap; this probably accounts for the consistently higher phage titers from strains containing pCTX-Kn. Transduction assays were performed as described in Table 1.
21. E. V. Koonin, *FEBS Lett.* **312**, 3 (1992).
22. A. P. Pugsley and O. Francetic, *Cell Mol. Life Sci.* **54**, 347 (1998).
23. M. Lindeberg, G. P. Salmund, A. Collmer, *Mol. Microbiol.* **20**, 175 (1996).
24. M. Lessl et al., *J. Bacteriol.* **174**, 2493 (1992).
25. M. Sandkvist, M. Bagdasarian, S. P. Howard, V. J. DiRita, *EMBO J.* **14**, 1664 (1995).
26. M. Sandkvist, L. P. Hough, M. M. Bagdasarian, M. Bagdasarian, *J. Bacteriol.* **181**, 3129 (1999).
27. We thank M. Russel, A. Camilli, A. L. Sonenshein, and Waldor lab colleagues for helpful suggestions and critical reading of the manuscript and A. Kane and the New England Medical Center GRASP Center for preparation of plates and media. S.S. thanks G. Morris and J. Johnson for research support. This work was supported by NIH grant AI-42347 to M.K.W. M.K.W. is a Pew Scholar in the Biomedical Sciences. M.S. was supported by funds from the American Red Cross. S.S. was supported by a University of Maryland Intramural Grant.

23 November 1999; accepted 25 February 2000

## Functional Role of Caspase-1 and Caspase-3 in an ALS Transgenic Mouse Model

Mingwei Li,<sup>1</sup> Victor O. Ona,<sup>1</sup> Christelle Guégan,<sup>2</sup> Minghua Chen,<sup>1</sup> Vernice Jackson-Lewis,<sup>2</sup> L. John Andrews,<sup>1</sup> Adam J. Olszewski,<sup>1</sup> Philip E. Stieg,<sup>1</sup> Jean-Pyo. Lee,<sup>4</sup> Serge Przedborski,<sup>2,3</sup> Robert M. Friedlander<sup>1\*</sup>

Mutations in the copper/zinc superoxide dismutase (SOD1) gene produce an animal model of familial amyotrophic lateral sclerosis (ALS), a fatal neurodegenerative disorder. To test a new therapeutic strategy for ALS, we examined the effect of caspase inhibition in transgenic mice expressing mutant human SOD1 with a substitution of glycine to alanine in position 93 (mSOD1<sup>G93A</sup>). Intracerebroventricular administration of zVAD-fmk, a broad caspase inhibitor, delays disease onset and mortality. Moreover, zVAD-fmk inhibits caspase-1 activity as well as caspase-1 and caspase-3 mRNA up-regulation, providing evidence for a non-cell-autonomous pathway regulating caspase expression. Caspases play an instrumental role in neurodegeneration in transgenic mSOD1<sup>G93A</sup> mice, which suggests that caspase inhibition may have a protective role in ALS.

ALS is a neurodegenerative disorder involving motor neuron loss in the brain, brainstem, and spinal cord and resulting in progressive paralysis. ALS is universally fatal, with an average mortality of 5 years after onset (1).

Familial ALS accounts for 10 to 20% of all cases; the remaining cases are sporadic. Both forms of the disease have indistinguishable clinical and histopathological features (2). Mutations of the SOD1 (mSOD1) gene have been identified in some cases of familial ALS (3, 4). Transgenic mice have been generated expressing different mSOD1 genes identified in ALS patients (5, 6). Like humans with ALS, these mice develop an adult-onset progressive motor deterioration universally leading to early death and have been used as models for the disease (5, 7). Although the mechanisms leading to motor neuron degen-

<sup>1</sup>Neuroapoptosis Laboratory and Neurosurgical Service, Department of Surgery, Brigham and Women's Hospital, Harvard Medical School, Boston, MA 02115, USA. <sup>2</sup>Department of Neurology, <sup>3</sup>Department of Pathology, Columbia University, New York, NY 10032, USA. <sup>4</sup>Department of Medicine, University of Chicago, Chicago, IL 60637, USA.

\*To whom correspondence should be addressed. E-mail: rfriedlander@rics.bwh.harvard.edu

## REPORTS

eration in ALS are not thoroughly understood, evidence points to apoptotic pathways playing a role in human and mouse models of the disease (8–10). The caspase family plays an important role in the pathogenesis of central nervous system (CNS) disorders featuring apoptosis (11–17). Recent reports provide evidence for caspase-3 activation in human ALS (18). In addition, mSOD1 expression induces caspase-dependent neuronal apoptosis *in vitro* (19). The importance of apoptotic pathways in the pathogenesis of ALS is supported by the neuroprotective effects of both the Bcl-2 transgene and the dominant-negative caspase-1 inhibitor transgene in transgenic mSOD1<sup>G93A</sup> mice (9, 10). Evidence exists of caspase-1 and caspase-3 activation in ALS mice (20). Here we provide direct evidence for a functional role of caspase-1 and caspase-3 in presymptomatic and end-stage mSOD1<sup>G93A</sup> mice and demonstrate a therapeutic benefit of pharmacologic caspase inhibition (21). In addition, we demonstrate that caspase-1 is activated in the human ALS spinal cord.

Because caspase-1 activity has been detected in spinal cords of mSOD1<sup>G93A</sup> mice and caspase-3 activity has been detected in the same mice and in humans with ALS, we evaluated the expression of activated caspase-1 and caspase-3 in spinal motor neurons of mSOD1<sup>G93A</sup> mice (8, 20, 22). We performed double staining with a neuron-specific antibody

(NeuN) and either an antibody to activated caspase-1 or to activated caspase-3 (23). Beginning at 70 days of age and thereafter at 90 and 110 days, caspase-1 and caspase-3 staining were shown primarily in NeuN-positive cells in the ventral horn of the spinal cord of transgenic mSOD1<sup>G93A</sup> mice (Fig. 1, A through P). Caspase-positive NeuN-positive cells tended to be smaller than caspase-negative NeuN-positive cells, suggesting a more advanced apoptotic phenotype. Caspase-1 or caspase-3 staining was not detected in spinal cord sections of wild-type littermates or in the brain, spinal cord white matter, or dorsal horn of transgenic mSOD1<sup>G93A</sup> mice. We evaluated by Western blot the caspase-1 and caspase-3 antibodies used for immunostaining to confirm their specificity in spinal cord tissue for the activated caspase subunits (Fig. 1, Q and S). We compared spinal cord lysates of presymptomatic (50 days) and symptomatic (90 days) mSOD1<sup>G93A</sup> mice using other caspase-1 and caspase-3 antibodies that recognize both the procaspase and the cleaved activated subunit (Fig. 1, R and T). Activated caspase-1 and caspase-3 were detected in symptomatic mice and not in presymptomatic mice. In addition, the activated caspase antibodies specifically recognized the cleaved form of caspase-1 and caspase-3 and not the procaspase (Fig. 1, Q and S).

In light of the fact that caspase-1 and caspase-3 are activated in spinal cord motor

neurons of transgenic mSOD1<sup>G93A</sup> mice, we evaluated their functional contribution to the progression of the disease by pharmacologically inhibiting them. *N*-benzyloxycarbonyl-Val-Asp-fluoromethylketone (zVAD-fmk) was selected as the agent to be evaluated because it is a broad caspase inhibitor that is well tolerated by mice in prolonged administration protocols, and it has a proven efficacy in other neurodegenerative disease models (14). We used osmotic pumps for delivery of zVAD-fmk into the cerebral ventricle (24). Osmotic pumps were implanted into 60-day-old mice. At this age there has been no significant neuronal loss, clinically representing the late presymptomatic stage of the disease. Pumps continuously delivered the drug for 56 days. The onset of motor and/or coordination deficits was defined as the first day that a mouse could not remain on the Rotarod for 7 min at a speed of 20 rpm (25). Mortality was scored as the age of death or the age when the mouse was unable to right itself within 30 s. The length of time before disease onset in transgenic mice treated with either vehicle or 300  $\mu$ g of zVAD-fmk per 20 g of body weight for 28 days (300  $\mu$ g/20 g body weight/28 days) was  $103.5 \pm 2.8$  days and  $123.7 \pm 6.8$  days, respectively. zVAD-fmk delayed the disease-induced onset of Rotarod deficit by  $20.2 \pm 6.4$  days. In addition, zVAD-fmk treatment prolonged survival from  $126.1 \pm 3.0$  days to  $153.3 \pm 8.8$  days as compared with

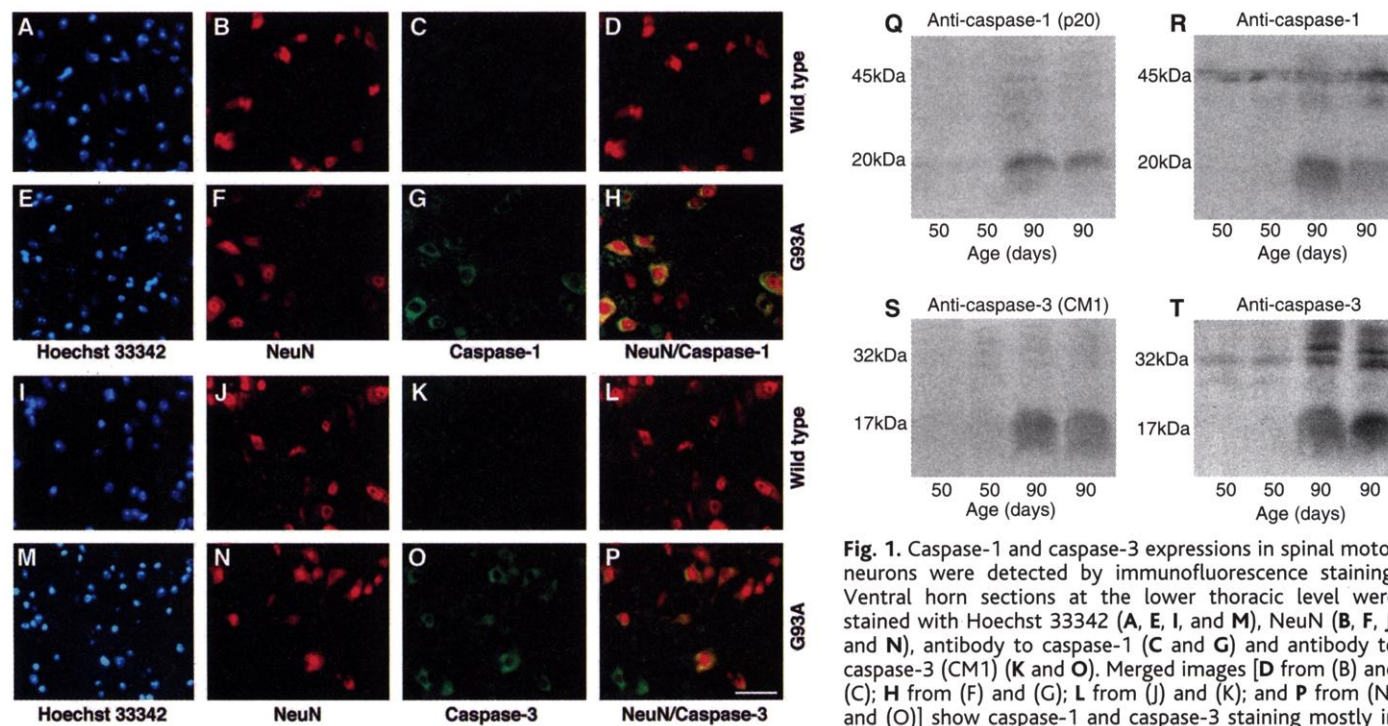


**Fig. 1.** Caspase-1 and caspase-3 expressions in spinal motor neurons were detected by immunofluorescence staining. Ventral horn sections at the lower thoracic level were stained with Hoechst 33342 (A, E, I, and M), NeuN (B, F, J, and N), antibody to caspase-1 (C and G) and antibody to caspase-3 (CM1) (K and O). Merged images [D from (B) and (C); H from (F) and (G); L from (J) and (K); and P from (N) and (O)] show caspase-1 and caspase-3 staining mostly in NeuN-positive but also in NeuN-negative cells, demonstrating

induction of both caspases in mSOD1 mice. No caspase-1 or caspase-3 staining was detected in the dorsal horn or in spinal cord sections from wild-type littermates [(C) and (K)]. The staining is representative of 70-, 90-, and 110-day-old wild-type and mSOD1 mice ( $n = 3$  mice per group). Scale bar, 30  $\mu$ m. (Q through T) Western blot of lysates from 50- and 90-day-old mSOD1<sup>G93A</sup> mice. (Q) Activated caspase-1 antibody (p20) used in the immunostaining; (R) caspase-1 antibody, which recognizes procaspase-1 (p45) and activated caspase-1; (S) activated caspase-3 antibody (p17) used in the immunostaining; and (T) caspase-3 antibody, which recognizes procaspase-3 (p32) and activated caspase-3. Each lane was loaded with 50  $\mu$ g of protein.

REPORTS

vehicle-treated littermates, representing a lifespan prolonged by 22% (Fig. 2, A through C). zVAD-fmk-mediated neuroprotection was dose-dependent because mice treated with a lower dose (100  $\mu\text{g}/20\text{ g}$  body weight/28 days) survived 11% longer than vehicle-treated mice. However, this protection did not reach statistical significance. Motor strength and coordination, as evaluated by Rotarod performance, were significantly improved in zVAD-fmk-treated mice (Fig. 2, D through F).

A hallmark of ALS in humans, as well as in mSOD1<sup>G93A</sup> transgenic mice, is a progressive loss of spinal motor neurons (2, 5, 6). To evaluate the effect of zVAD-fmk on motor neuron loss, we compared the numbers of cervical and lumbar motor neurons in both zVAD-fmk- and vehicle-treated mSOD1<sup>G93A</sup> mice at 110 days of age (26). At this stage, vehicle-treated mice are at the end stage of the disease. zVAD-fmk-treated mice had a significantly greater number of motor neurons at the cervical level as compared with vehicle-treated mice (Fig. 3A). At the lumbar level, zVAD-fmk-treated mice also had a greater number of motor neurons; however, this did not reach statistical significance (Fig. 3B). The greater protection from motor neuron loss at the cervical level likely represents a zVAD-fmk concentration effect. Because zVAD-fmk is delivered to the cerebral ventricle, the concentration reaching cervical motor neurons is higher than in the lumbar area, demonstrating a concentration-dependent effect of

zVAD-fmk neuroprotection. Degeneration of phrenic nerve axons was also significantly inhibited in zVAD-fmk-treated mice (Fig. 3C). zVAD-fmk extends survival of mSOD1 mice by inhibiting motor neuron cell death.

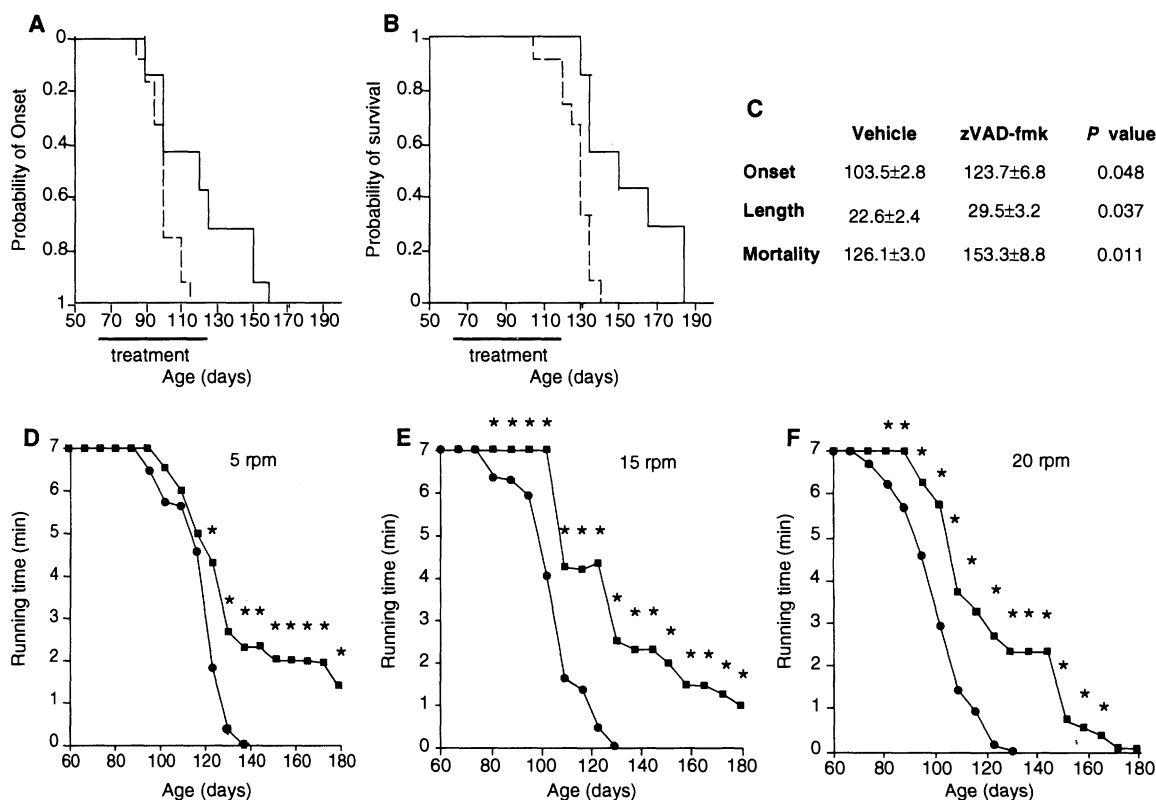
Given that caspase-1 is activated in the spinal cords of mSOD1<sup>G93A</sup> mice, we evaluated whether zVAD-fmk inhibits caspase-1 activity (22). Detection of mature interleukin 1- $\beta$  (IL-1 $\beta$ ) has been used as a sensitive and specific marker of caspase-1 activation (11–14, 27). Mature IL-1 $\beta$  levels were 2.4-fold higher in spinal cord samples of 100-day-old mSOD1<sup>G93A</sup> mice when compared with age-matched wild-type littermates, indicating caspase-1 activation (28). zVAD-fmk treatment resulted in a 37% reduction of caspase-1 activity in the spinal cords of mSOD1<sup>G93A</sup> mice (Fig. 3D). We next evaluated whether caspase-1 activation is also detected in the spinal cords of humans with ALS. We demonstrated an 81.5% elevation of caspase-1 activity in the spinal cord of humans with ALS when compared with normal controls (Fig. 3E). These results further validate this mouse as a relevant disease model. Because mature IL-1 $\beta$  plays a functional role in neuronal cell death, zVAD-fmk-mediated neuroprotection in mSOD1 mice is likely mediated in part by inhibiting activation of this cytokine (19, 29, 30).

Because increased caspase-1 and caspase-3 activity in transgenic mSOD1<sup>G93A</sup> mice has been demonstrated, we investigated whether

these caspases might also be regulated at the transcription level (20, 22). Using reverse transcriptase-polymerase chain reaction (RT-PCR), we quantified caspase-1 and caspase-3 mRNA expression in transgenic mSOD1<sup>G93A</sup> mice and evaluated the effect of caspase inhibition on their expression (31). Beginning at 70 days of age, caspase-1 mRNA levels began to increase, peaking at 3.2-fold above wild-type levels at 90 days (Fig. 4, A and B). Caspase-3 mRNA elevation began at 90 days of age and peaked at 110 days with levels 2.6-fold above those in the wild-type mice (Fig. 4, C and D). Caspase-1 and caspase-3 mRNA levels were significantly reduced in zVAD-fmk-treated mice by 27 and 34%, respectively, as compared with vehicle-treated mSOD1 littermates.

zVAD-fmk is an enzymatic caspase inhibitor. However, decreased caspase mRNA expression levels mediated by zVAD-fmk are consistent with a detrimental role of intracellular and extracellular diffusible factors resulting from caspase activation (19, 30). Caspase inhibition decreases the production of diffusible factors such as mature IL-1 $\beta$  and free radicals (11–14). In addition, blocking extracellular binding of endogenously produced IL-1 $\beta$  inhibits cell death, suggesting a proapoptotic role of extracellular caspase downstream mediators (19, 30). Furthermore, direct injection of IL-1 $\beta$  into the rat brain induces neuronal apoptosis (32). As in human neurodegeneration, cell loss in mSOD1 mice is not synchronized—it occurs over a pro-

**Fig. 2.** Cumulative probability of onset of Rotarod deficits (A) and survival (B) in mSOD1 mice. Survival was significantly prolonged and the onset of Rotarod deficit was significantly delayed in mSOD1 mice treated with zVAD-fmk when compared with vehicle-treated transgenic littermates. Solid line, zVAD-fmk; dashed line, vehicle. (C) Table of onset of motor deficit and mortality. Motor function was tested with the Rotarod at 5 (D), 15 (E), and 20 rpm (F). Testing was terminated either when the mice fell from the rod or at 7 min if the mouse remained on the rod. Mice treated with zVAD-fmk performed significantly better than vehicle-treated mice (\* $P < 0.05$ ; vehicle,  $n = 12$  mice; zVAD-fmk,  $n = 7$  mice). Square, zVAD-fmk; circle, vehicle.



longed period of time. Therefore, because neighboring cells are at different stages of the apoptotic pathway, diffusible factors produced by cells in which caspases are activated likely have a detrimental effect on neighboring cells,

resulting in caspase up-regulation. Hence, caspase inhibition in one cell likely delays a neighboring cell from initiating the caspase cascade. Thus, unlike in *Caenorhabditis elegans*, the caspase cascade in vertebrates is not cell-auton-

omous but rather is influenced in a paracrine fashion by the extracellular microenvironment (33).

We demonstrate inhibition of disease progression and extended survival in a transgenic mouse model of ALS by pharmacologic caspase inhibition, and we show that caspase-1 and caspase-3 are expressed in neurons in transgenic mSOD1<sup>G93A</sup> mice. Furthermore, we demonstrate that caspase-1 is activated in spinal cord samples from humans affected by ALS. Consistent with in vitro evidence in nonneuronal cell lines, we demonstrate that caspase-1 mRNA is up-regulated before that of caspase-3, suggesting that caspase-1 mediates early disease processes and that caspase-3 may be involved in the terminal stage of the apoptotic pathway (34, 35). Interestingly, in vitro caspase-1 activates caspase-3 (36). In addition to an inflammatory role of caspase-1, early caspase-1 neuronal expression indicates its importance as an early mediator of the neuronal apoptotic cascade. Because of the extensive similarities in the behavioral, histologic, and molecular mechanisms between the mSOD1<sup>G93A</sup> transgenic mouse and humans with ALS (familial and sporadic), these results provide therapeutic information relevant to the human disease. These results indicate that caspases play a role not only in the end stage of ALS but also in the presymptomatic progression of the disease, which suggests that therapy targeted at inhibiting caspase function should begin in the presymptomatic stage of ALS.

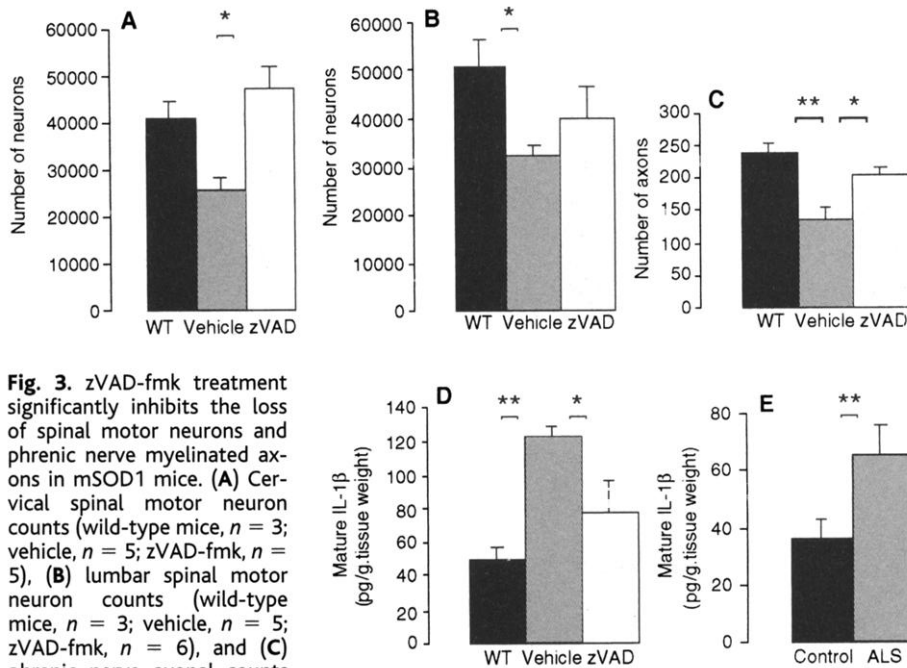


**Fig. 3.** zVAD-fmk treatment significantly inhibits the loss of spinal motor neurons and phrenic nerve myelinated axons in mSOD1 mice. (A) Cervical spinal motor neuron counts (wild-type mice,  $n = 3$ ; vehicle,  $n = 5$ ; zVAD-fmk,  $n = 5$ ), (B) lumbar spinal motor neuron counts (wild-type mice,  $n = 3$ ; vehicle,  $n = 5$ ; zVAD-fmk,  $n = 6$ ), and (C) phrenic nerve axonal counts ( $n = 6$  mice per group) in 110-day old mice. Mature IL-1 $\beta$  levels, indicating caspase-1 activation in (D) mSOD1 mice at 100 days of age ( $n = 4$  mice per group) and in (E) human spinal cord normal control and ALS patients ( $n = 4$  humans per group). Mature IL-1 $\beta$  levels significantly increased in mSOD1 transgenic mice and in human ALS patients as compared with wild-type age-matched littermates and control spinal cord tissue. zVAD-fmk treatment reduced caspase-1 activity in the spinal cords of mSOD1 mice ( $*P < 0.05$ ,  $**P < 0.01$ ). Error bars indicate SEM.

References and Notes

1. D. B. Williams and J. A. Windebank, *Peripheral Neuropathy*, P. J. Dyck, P. K. Thoma, J. W. Griffin, P. A. Low, J. F. Poduslo, Eds. (Saunders, Philadelphia, ed. 3, 1993).
2. L. P. Rowland, in *Merritt's Textbook of Neurology*, L. P. Rowland, Ed. (Williams & Wilkins, Philadelphia PA, 1995), pp. 742-749.
3. D. R. Rosen et al., *Nature* **362**, 59 (1993).
4. H. X. Deng et al., *Science* **261**, 1047 (1993).
5. M. E. Gurney et al., *Science* **264**, 1772 (1994).
6. D. R. Borchelt et al., *Neurobiol. Dis.* **5**, 27 (1998).
7. M. E. Gurney, T. J. Fleck, C. S. Himes, E. D. Hall, *Neurology* **50**, 62 (1998).
8. L. J. Martin, *J. Neuropathol. Exp. Neurol.* **58**, 459 (1999).
9. R. M. Friedlander, R. H. Brown, V. Gagliardini, J. Wang, J. Yuan, *Nature* **388**, 31 (1997).
10. V. Kostic, V. Jackson-Lewis, F. de Bilbao, M. Dubois-Dauphin, S. Przedborski, *Science* **277**, 559 (1997).
11. H. Hara et al., *Proc. Natl. Acad. Sci. U.S.A.* **94**, 2007 (1997).
12. K. B. Fink et al., *Neuroscience* **94**, 1213 (1999).
13. R. M. Friedlander et al., *J. Exp. Med.* **185**, 933 (1997).
14. V. O. Ona et al., *Nature* **399**, 263 (1999).
15. S. Namura et al., *J. Neurosci.* **18**, 3659 (1998).
16. J. E. Springer, R. D. Azbill, P. E. Knapp, *Nature Med.* **5**, 943 (1999).
17. A. G. Yakovlev et al., *J. Neurosci.* **17**, 7415 (1997).
18. L. J. Martin, A. C. Price, A. Kaiser, A. Y. Shaikh, Z. Liu, *Int. J. Mol. Med.* **5**, 3 (2000).
19. C. M. Troy, L. Stefanis, A. Prochiantz, L. A. Greene, M. L. Shelanski, *Proc. Natl. Acad. Sci. U.S.A.* **93**, 5635 (1996).
20. S. Vukosavic, L. Stefanis, S. Przedborski, *Soc. Neurosci. Abstr.* **25**, 1304 (1999).
21. Male transgenic mice expressing the human mSOD1<sup>G93A</sup> were bred with background-matched B6SJL wild-type females (Jackson Laboratories, Bar Harbor, ME). The progeny were genotyped and used

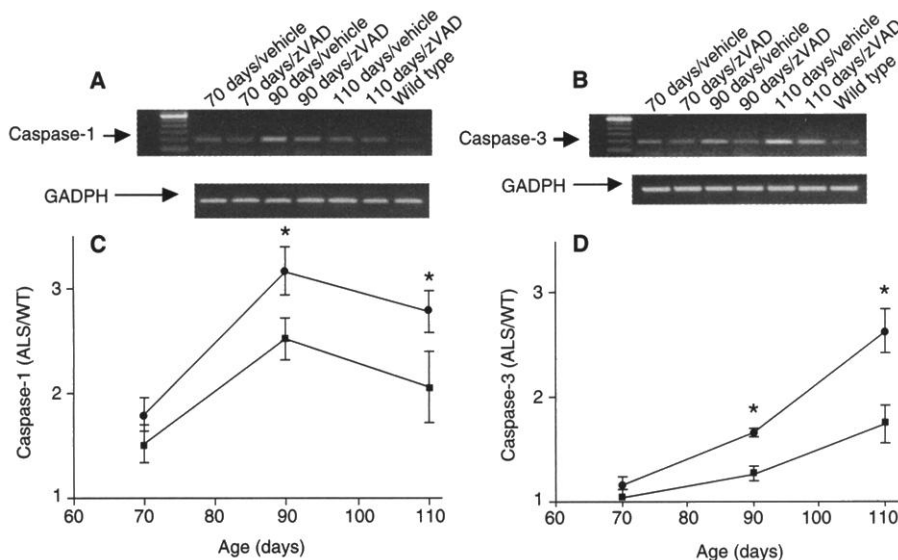


**Fig. 4.** Caspase-1 and caspase-3 mRNA levels were quantified in spinal cord specimens of mSOD1 mice. Ethidium bromide-stained gels of RT-PCR analysis of (A) caspase-1 and (B) caspase-3 mRNA run in parallel with those of GAPDH mRNA. (C) and (D) show time-dependent up-regulation of (C) caspase-1 and (D) caspase-3 mRNA expression in mSOD1 transgenic mice compared with age-matched wild-type mice ( $*P > 0.05$ ,  $n = 6$  mice per time point). Caspase levels are normalized to GAPDH expression and tabulated as the caspase ratio of SOD<sup>G93A</sup> to wild-type mice. Square, zVAD-fmk; circle, vehicle. Error bars indicate SEM.

- for subsequent studies. Experiments were conducted in accordance with protocols approved by the Harvard Medical School Animal Care Committee.
22. P. Pasinelli, D. R. Borchelt, M. K. Houseweart, D. W. Cleveland, R. H. Brown Jr., *Proc. Natl. Acad. Sci. U.S.A.* **95**, 15763 (1998).
  23. To investigate whether caspase-1 and caspase-3 are activated in the mSOD1 mouse spinal cord, we performed immunohistochemical staining with an antibody specific for activated caspase-1 (provided by J. Yuan, Harvard Medical School, Boston, MA) and an antibody specific to activated caspase-3, which is also known as CM1 (provided by A. Srinivasan, Idun Pharmaceutical, La Jolla, CA). In addition, a neuron-specific marker, anti-NeuN antibody (Chemicon, Temecula, CA), was used in a double staining procedure to identify neuronal cells. At 70, 90, and 110 days of age, mice were killed and perfused with 4% paraformaldehyde. Spinal cords were removed under a dissecting microscope. Tissue was frozen in cold isopentane after cryoprotection in 30% sucrose. Frozen sections (10  $\mu$ m thick) were washed with phosphate-buffered saline (PBS) containing 0.05% Tween-20 and were incubated with 5% normal goat serum. The sections were incubated overnight with rat polyclonal antibody to caspase-1 (1:5) or rabbit polyclonal antibody to caspase-3 (CM1) (1:2000), washed overnight, then washed three times with PBS, and finally probed with a biotinylated secondary antibody to rat immunoglobulin G (IgG) or a biotinylated secondary antibody to rabbit IgG (1:300; Vector, Burlingame, CA) for 2 hours. Next, specimens were incubated in Fluorescein Avidin DCS (1:1000; Vector). Sections were also double stained with the NeuN antibody (1:100) followed by Texas Red antibody to mouse (1:200; Vector). Hoechst 33342 was used for counterstaining. The fluorescent stained sections were evaluated with epifluorescence microscopy.
  24. At 60 days of age, osmotic pumps (Alzet, Palo Alto, CA) were used for the intracerebroventricular delivery of zVAD-fmk (Enzyme Systems, Livermore, CA). Pumps were filled with vehicle (0.4% dimethyl sulfoxide, 0.1 M Pipes, pH 6.9), 100  $\mu$ g of 2 VAG-fmk per 20g body weight, or 300  $\mu$ g of zVAG-fmk per 20 g of body weight. Pumps continuously delivered the drug for 28 days and were then exchanged for new pumps filled with fresh drug or vehicle for an additional 28-day treatment. The investigator was blind to the identity of the drug or vehicle used in the pump until the death of all mice.
  25. A Rotarod (Columbus Instruments, Columbus, OH) was used to evaluate motor function. Mice were first evaluated the day before placement of the osmotic pumps and thereafter on a weekly basis. Mice were placed on the rotating rod at speeds of 5, 15, and 20 rpm. The time each mouse remained on the rod was registered automatically. If the mouse remained on the rod for 7 min, the test was completed and scored as 7 min.
  26. Spinal cord and phrenic nerve samples were collected and processed as described (10). Motor neurons were counted on cryostat-cut sections (40  $\mu$ m thick) stained with thionin. Quantification was performed by stereology as described by Liberatore *et al.* [*Nature Med.* **5**, 1403 1999] on every 10th spinal cord section, spanning the entire cervical and lumbar enlargements.
  27. K. Kuida *et al.*, *Science* **267**, 2000 (1995).
  28. Mature IL-1 $\beta$  concentration was measured with an enzyme-linked immunosorbent assay (ELISA) kit (R&D, Minneapolis, MN), which is specific for the mature form of the cytokine. Full-length spinal cord tissue was removed from mice treated with zVAD-fmk or vehicle at 100 days of age. Tissue was processed as previously described (20). Human spinal cord samples were generously provided by the Harvard, Massachusetts General Hospital, and Columbia brain banks.
  29. R. M. Friedlander and J. Yuan, *Cell Death Differ.* **5**, 823 (1998).
  30. R. M. Friedlander, V. Gagliardini, R. J. Rotello, J. Yuan, *J. Exp. Med.* **184**, 717 (1996).
  31. Spinal cord tissue was obtained from 70-, 90-, and 110-day-old mice. Total RNA was extracted with Trizol (Life Technologies, Rockville, MD), and 1 mg was used as a template for first-strand synthesis. Primers were designed from published sequences (Life Technologies). Primers used to amplify caspase-1 were 5'-TGG TCT TGT GAC TTG GAG GA-3' and 5'-TGG CTT CTT ATT GGC ACG AT-3', resulting in a 191-base pair (bp) amplified product. For caspase-3, primer sequences were 5'-TGT CAT CTC GCT CTG GTA CG-3' and 5'-AAA TGA CCC CTT CAT CAC CA-3', resulting in a 200-bp amplified product. To confirm cDNA integrity and to standardize expression levels, we amplified fragments of glyceraldehyde phosphate-3-dehydrogenase (GAPDH) in parallel. Products were analyzed by electrophoresis in a 1.5% agarose gel and were visualized by ethidium bromide staining. A Chemi Doc imaging system (BioRad) was used for signal quantification. Signals are expressed as the ratio of band densities (caspase/GAPDH) of caspase expression in ALS and wild-type mice.
  32. S. Holmin and T. Mathiesen, *J. Neurosurg.* **92**, 108 (2000).
  33. J. Y. Yuan and H. R. Horvitz, *Dev. Biol.* **138**, 33 (1990).
  34. M. Enari, R. V. Talanian, W. W. Wong, S. Nagata, *Nature* **380**, 723 (1996).
  35. A. Ali *et al.*, *J. Hematother. Stem Cell Res.* **8**, 343 (1999).
  36. M. Tewari *et al.*, *Cell* **81**, 801 (1995).
  37. We thank A. Srinivasan for providing the CM1 antibody and J. Yuan for providing the caspase-1 antibody; M. Schoenebeck for expert preparation of the phrenic nerve samples; J. Yuan for insightful comments on the manuscript; and E. Friedlander for editorial assistance. Supported by the Muscular Dystrophy Association; the ALS Association; Project-ALS; the National Institute of Neurological Disorders and Stroke (grants R01 NS38586, R29 NS37345, and P50 NS38370); the U.S. Department of Defense (grant DAMD 17-99-1-9471); the Lowenstein Foundation; the Smart Foundation; and the Parkinson's Disease Foundation. C.G. is the recipient of a scholarship from the French ISERM. S.P. is a recipient of the Cotzias Award from the American Parkinson Disease Association.

4 February 2000; accepted 15 March 2000

## The Outcome of Acute Hepatitis C Predicted by the Evolution of the Viral Quasispecies

Patrizia Farci,<sup>1,2\*</sup> Atsushi Shimoda,<sup>3</sup> Alessandra Coiana,<sup>1</sup> Giacomo Diaz,<sup>4</sup> Giovanna Peddis,<sup>1</sup> Jacqueline C. Melpolder,<sup>5</sup> Antonello Strazzer,<sup>1</sup> David Y. Chien,<sup>6</sup> Santiago J. Munoz,<sup>7</sup> Angelo Balestrieri,<sup>1</sup> Robert H. Purcell,<sup>2</sup> Harvey J. Alter<sup>5</sup>

The mechanisms by which hepatitis C virus (HCV) induces chronic infection in the vast majority of infected individuals are unknown. Sequences within the HCV *E1* and *E2* envelope genes were analyzed during the acute phase of hepatitis C in 12 patients with different clinical outcomes. Acute resolving hepatitis was associated with relative evolutionary stasis of the heterogeneous viral population (quasispecies), whereas progressing hepatitis correlated with genetic evolution of HCV. Consistent with the hypothesis of selective pressure by the host immune system, the sequence changes occurred almost exclusively within the hypervariable region 1 of the *E2* gene and were temporally correlated with antibody seroconversion. These data indicate that the evolutionary dynamics of the HCV quasispecies during the acute phase of hepatitis C predict whether the infection will resolve or become chronic.

HCV infection is an important public health problem worldwide (1) because it is a major cause of chronic hepatitis, cirrhosis, and hepatocellular carcinoma (2). Very rarely, HCV causes fulminant hepatitis (FH), the most severe

form of acute hepatitis. Although the infection resolves in 15% of cases, it becomes chronic in up to 85% of infected individuals (3). The clinical course of chronic hepatitis C is highly variable. In about 70% of the patients the disease is mild and stable over several decades, whereas in the remaining 30% it is more rapidly progressive. Prospective studies of hepatitis C have failed to identify any clinical, serologic, or virologic features that predict the outcome of the disease (4).

The mechanisms responsible for the high rate of viral persistence and for the variable clinical course of hepatitis C are unknown, but are thought to represent a complex interplay between viral diversity and host immunity (5). Although HCV infection induces strong cellular and humoral immune responses (6, 7), they are generally insufficient to

<sup>1</sup>Department of Medical Sciences, University of Cagliari, Via San Giorgio 12, 09124 Cagliari, Italy. <sup>2</sup>Hepatitis Viruses Section, Laboratory of Infectious Diseases, National Institute of Allergy and Infectious Diseases, National Institutes of Health (NIH), Bethesda, MD 20892, USA. <sup>3</sup>Department of Internal Medicine, Kanazawa University, Kanazawa 920-8641, Japan. <sup>4</sup>Department of Cytomorphology, University of Cagliari, 09124 Cagliari, Italy. <sup>5</sup>Department of Transfusion Medicine, Warren G. Magnuson Clinical Center, NIH, Bethesda, MD 20892, USA. <sup>6</sup>Chiron Corporation, Emeryville, CA 94507, USA. <sup>7</sup>Albert Einstein Medical Center, Philadelphia, PA 19141, USA.

\*To whom correspondence should be addressed. E-mail: farcip@pacs.unica.it-